

Gradient Flow Renormalisation for Meson Mixing and Lifetimes

Matthew Black,^{a,1,*} Robert Harlander,^b Fabian Lange,^{c,d} Antonio Rago,^e Andrea Shindler^{b,f,g} and Oliver Witzel^a

^a*Center for Particle Physics Siegen, Theoretische Physik 1, Naturwissenschaftlich-Technische Fakultät, Universität Siegen, 57068 Siegen, Germany*

^b*Institute for Theoretical Particle Physics and Cosmology, RWTH Aachen University, 52056 Aachen, Germany*

^c*Physik-Institut, Universität Zürich, Winterthurerstrasse 190, 8057 Zürich, Switzerland*

^d*PSI Center for Neutron and Muon Sciences, 5232 Villigen PSI, Switzerland*

^e*IMADA and Quantum Theory Center, University of Southern Denmark, Odense, Denmark*

^f*Nuclear Science Division, Lawrence Berkeley National Laboratory, Berkeley, CA 94720, USA*

^g*Department of Physics, University of California, Berkeley, CA 94720, USA*

E-mail: matthew.black@uni-siegen.de

Fermionic gradient flow in combination with the short-flow-time expansion provides a computational method where the renormalisation of hadronic matrix elements on the lattice can be simplified to address e.g. the issue that operators with different mass dimension can mix.

We demonstrate our gradient flow renormalisation procedure by determining matrix elements of four-quark operators describing neutral meson mixing or meson lifetimes. While meson mixing calculations are well-established on the lattice and serve to validate our procedure, a lattice calculation of matrix elements for heavy meson lifetimes is still outstanding. Preliminary results for mesons formed of a charm and strange quark are presented.

The 41st International Symposium on Lattice Field Theory (Lattice 2024)

July 28th - August 3rd, 2024

Liverpool, UK

Preprints: SI-HEP-2024-21, P3H-24-067, ZU-TH 46/24, PSI-PR-24-19, TTK-24-37

¹Present address: School of Physics and Astronomy, University of Edinburgh, Edinburgh EH9 3JZ, UK

*Speaker

1. Introduction

The phenomenology of B mesons is a well-studied area at many collider experiments [1], with an impressive increase in precision of the measured properties of B mesons [2]. To fully leverage experimental results, theoretical predictions need to reach a similar precision. Of critical importance is to improve the precision of non-perturbative parameters. These can e.g. be calculated in terms of hadronic matrix elements using lattice QCD. Matrix elements of four-quark dimension-six operators are important in further constraining the behaviour of neutral meson mixing and also predicting the lifetime of a B meson via the heavy quark expansion (HQE).

The calculation of short-distance $\Delta Q = 2$ (for generic heavy quark Q) operators governing neutral meson mixing is well established on the lattice for both charm [3–5] and bottom [6–11] sectors. The $\Delta Q = 0$ matrix elements relevant for lifetime predictions have received less attention on the lattice. There exist early quenched [12, 13] and preliminary unquenched [14] results from the turn of the millennium, however nothing else for many years until more recently [15–17]. While some of the calculation follows similarly to the case of the $\Delta Q = 2$ operators, the $\Delta Q = 0$ operators additionally require disconnected and ‘eye’ diagrams where the statistical noise is much larger. Furthermore, mixing with operators of lower mass dimension arises under renormalisation.

In the following, we study the gradient flow (GF) [18–20] as a non-perturbative tool to simplify the renormalisation procedure in lattice calculations. We match the results at finite flow time, τ , to the $\overline{\text{MS}}$ scheme using the short-flow-time expansion (SFTX) [21–23] where the matching coefficients ζ^{-1} are calculated perturbatively [24–27]. We first test our method using the $\Delta Q = 2$ matrix elements where findings can be validated against the literature, and then show first results towards a lattice calculation of the $\Delta Q = 0$ matrix elements.

2. Lattice calculation

We use six RBC/UKQCD 2+1-flavour domain-wall fermion (DWF) and Iwasaki gauge ensembles with three lattice spacings $a \sim 0.11, 0.08, 0.07$ fm and $267 \text{ MeV} \leq m_\pi \leq 433 \text{ MeV}$ as determined by RBC/UKQCD [28–30]. These ensembles are listed in Table 1. Light and strange quarks are simulated with the Shamir kernel of the DWF action [31–34] with $M_5 = 1.8$.

	L	T	a^{-1}/GeV	am_l^{sea}	am_s^{sea}	am_c^{val}	m_π/MeV	$\text{srcs} \times N_{\text{conf}}$	σ	N_σ
C1	24	64	1.7848	0.005	0.040	0.64	340	32×101	4.5	400
C2	24	64	1.7848	0.010	0.040	0.64	433	32×101	4.5	400
M1	32	64	2.3833	0.004	0.030	0.45	302	32×79	6.5	400
M2	32	64	2.3833	0.006	0.030	0.45	362	32×89	6.5	100
M3	32	64	2.3833	0.008	0.030	0.45	411	32×68	6.5	100
F1S	48	96	2.785	0.002144	0.02144	0.37	267	24×98		

Table 1: RBC/UKQCD ensembles used in the discussed simulations [28, 29, 35, 36]. am_l^{sea} and am_s^{sea} are the light and strange sea quark masses and m_π is the unitary pion mass. am_s^{val} are the valence strange quark masses, set to the physical mass.

Heavy quarks are simulated using stout-smeared gauge fields [37] and the Möbius kernel of the DWF action [38] with parameters $b = 1.5$ and $c = 0.5$, where the mass has been tuned to the physical charm mass on each ensemble through the D_s pseudoscalar meson [39]. Using a similar setup as Ref. [30], all propagators are generated with Z2-noise wall sources to which we apply Gaussian smearing for the strange quarks on the C and M ensembles. The number of sources and smearing parameters are listed in Table 1. Measurements were performed using Grid [40, 41] and Hadrons [42].

The operators and their bag parameters considered are

$$\Delta Q = 2 : Q_1 = (\bar{q}\gamma_\mu(1 - \gamma_5)Q)(\bar{q}\gamma_\mu(1 - \gamma_5)Q), \quad B_1^{\Delta Q=2} = \frac{\langle P|Q_1|P \rangle}{\eta m^2 f^2}, \quad (1)$$

$$\Delta Q = 0 : O_1 = (\bar{Q}\gamma_\mu(1 - \gamma_5)q)(\bar{q}\gamma_\mu(1 - \gamma_5)Q), \quad B_1^{\Delta Q=0} = \frac{\langle P|O_1|P \rangle}{\eta m^2 f^2}, \quad (2)$$

$$T_1 = (\bar{Q}\gamma_\mu(1 - \gamma_5)T^a q)(\bar{q}\gamma_\mu(1 - \gamma_5)T^a Q), \quad \epsilon_1 = \frac{\langle P|T_1|P \rangle}{\eta m^2 f^2}, \quad (3)$$

where q indicates a light quark flavour and Q a heavy quark flavour. P is the pseudoscalar heavy-light meson formed from these with mass m and decay constant f . $\eta = \frac{8}{3}$ for Q_1 and 1 for O_1 and T_1 . For convenience in the lattice simulation, we choose a basis without the colour generator and relate back to the original operator T_1 in the parity-even projection, i.e.

$$T_1^+ = -\frac{1}{2}\tau_1^+ - \frac{1}{2N_c}O_1^+, \quad (4)$$

$$\tau_1 = (\bar{Q}\gamma_\mu(1 - \gamma_5)Q)(\bar{q}\gamma_\mu(1 - \gamma_5)q). \quad (5)$$

The ϵ_1 bag parameter is therefore not immediately available and is extracted via

$$\epsilon_1 = -\frac{1}{2}\epsilon_1^{\langle \tau_1 \rangle} - \frac{1}{2N_c}B_1^{\Delta Q=0}, \quad (6)$$

where the first term is the bag parameter of the τ_1 operator in the standard definition. The bag parameters of Q_1 , O_1 , and τ_1 are extracted from commonly-used ratios of three- and two-point functions; see e.g. Ref. [16]. The quark line diagrams for O_1 and τ_1 are shown in figure 1.

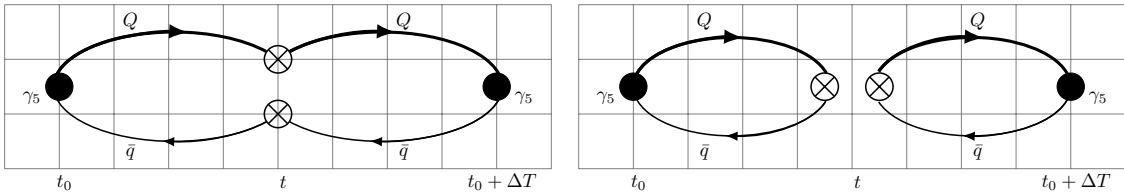


Figure 1: Quark line diagrams for the three-point correlation functions with $\Delta Q = 0$ four-quark operators inserted at time t between two sources at t_0 and $t_0 + \Delta T$ for O_1 (left) and τ_1 (right). The two $\Delta Q = 2$ diagrams for Q_1 follow similarly with charge inversion on one side of the operator insertion.

The $\Delta Q = 0$ operators have additional ‘eye’ diagram topologies which are computationally more challenging; see e.g. Ref. [43]. Since these are predicted to be small from sum rules [44], we do not yet consider them in this pilot study. Further, while the renormalisation at finite flow

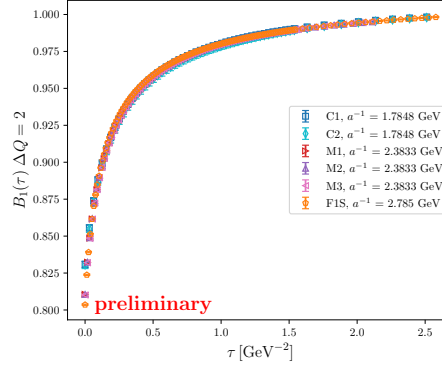


Figure 2: Flow time evolution of the bag parameter B_1 for $\Delta Q = 2$ in physical units τ [GeV^{-2}].

time is multiplicative, the matching to $\overline{\text{MS}}$ for the full $\Delta Q = 0$ operators involves mixing with lower-dimensional operators. At this stage we do not account for operator mixing and the matching uses a simplification valid for the difference of $\Delta Q = 0$ operators with different spectator quarks.

3. Results

3.1 Gradient Flow Evolution of Bag Parameters

Correlated fits are performed to extract bag parameters for each discrete flow time simulated. The evolution of the B_1 bag parameter for $\Delta Q = 2$ along the flow time is shown in figure 2, while the evolutions of the $\Delta Q = 0$ bag parameters B_1 and ϵ_1 are shown in figure 3. We see that the shape of evolution for ϵ_1 appears almost identical to that of $B_1^{\Delta Q=2}$, while $B_1^{\Delta Q=0}$ offers a different form. For all three quantities, we observe the following:

1. Data corresponding to different ensembles at the same lattice spacing but different light sea quark masses overlap. Hence we infer that sea quark effects are negligible;
2. There is also overlap of data determined on ensembles with different lattice spacings, which leads to the expectation that continuum limits will be very mild.

3.2 Continuum Limit

After linearly interpolating the values of the C and M ensembles from their own set of discrete flow times to values used on the F1S ensemble, we perform the continuum limit for each operator at each discrete flow time step using a linear ansatz in a^2 . Examples of the continuum limit extrapolations at two flow times are shown for the $B_1^{\Delta Q=2}$ bag parameter in figure 4, where we present one of the ‘flattest’ extrapolations on the left and one of the steeper extrapolations on the right. As suggested by the flow time evolution plots above, the continuum limits for the ϵ_1 bag parameter look very similar to these.

Examples of continuum limits for $B_1^{\Delta Q=0}$ are shown in figure 5. While the evolution in the flow time has a different functional form to the other parameters, we again find relatively mild continuum limits, where the plots shown represent some of the ‘steepest’ slopes found in the data.

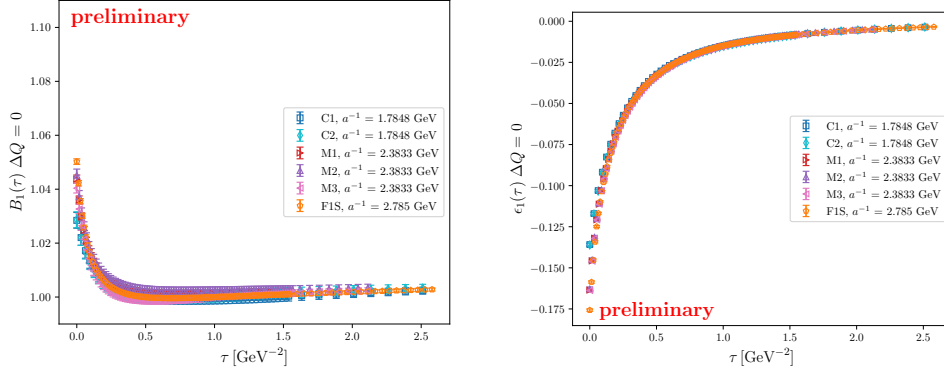


Figure 3: Flow time evolution of the $\Delta Q = 0$ bag parameters B_1 (left) and ϵ_1 (right) in physical units τ [GeV $^{-2}$].

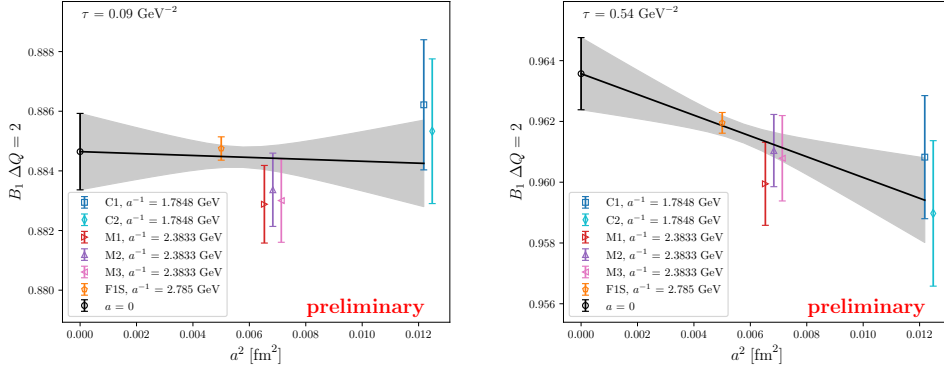


Figure 4: Examples of continuum limit extrapolations for the B_1 bag parameter for $\Delta Q = 2$ at flow times $\tau = 0.09$ GeV $^{-2}$ (left) and $\tau = 0.54$ GeV $^{-2}$ (right). For visibility, the M1 ensemble (red) is plotted with a slight offset to left, and the C2 (cyan) and M3 (pink) ensembles to the right.

3.3 Matching to $\overline{\text{MS}}$

Having performed the continuum limit for each flow time, the final step is to match these GF-renormalised results to the $\overline{\text{MS}}$ scheme. This is done by combining flowed operators with a perturbative matching matrix ζ^{-1} which leads to the $\overline{\text{MS}}$ result in the limit of $\tau \rightarrow 0$. The matching coefficients can be constructed from Refs. [24–27] through NNLO (in QCD). For $\Delta Q = 0$, the O_1 and T_1 operators mix such that both flowed operators contribute to the matched results. The $\tau \rightarrow 0$ limit will be taken assuming a linear extrapolation within an appropriate window in flow time. The flow time must be chosen sufficiently large that the data are not affected by large cut-off effects but also not too large such that the SFTX is still valid and higher-power effects remain negligible. Within the flow time window, currently an uncorrelated linear fit is performed and then extrapolated to $\tau = 0$. We take the difference between the fit of the central values and the fit to central values $\pm 1\sigma$ uncertainties to obtain the error on the extrapolated values. The renormalisation scale is fixed to be $\mu = 3$ GeV.

First we consider the $B_1^{\Delta Q=2}$ bag parameter combined with its perturbative matching in figure 6. We take the perturbative matching coefficient $\zeta_{B_1}^{-1}$ at both NLO and NNLO to study the systematic

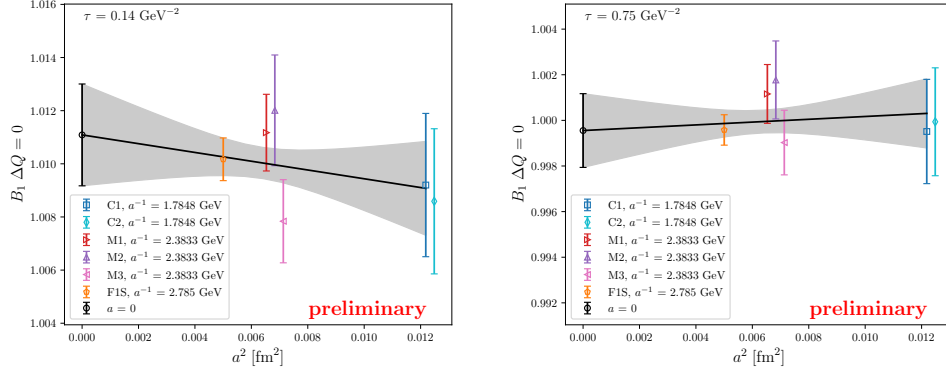


Figure 5: Examples of continuum limit extrapolations for the B_1 bag parameter for $\Delta Q = 0$ at flow times $\tau = 0.14 \text{ GeV}^{-2}$ (left) and $\tau = 0.75 \text{ GeV}^{-2}$ (right). For visibility, the M1 ensemble (red) is plotted with a slight offset to left, and the C2 (cyan) and M3 (pink) ensembles to the right.

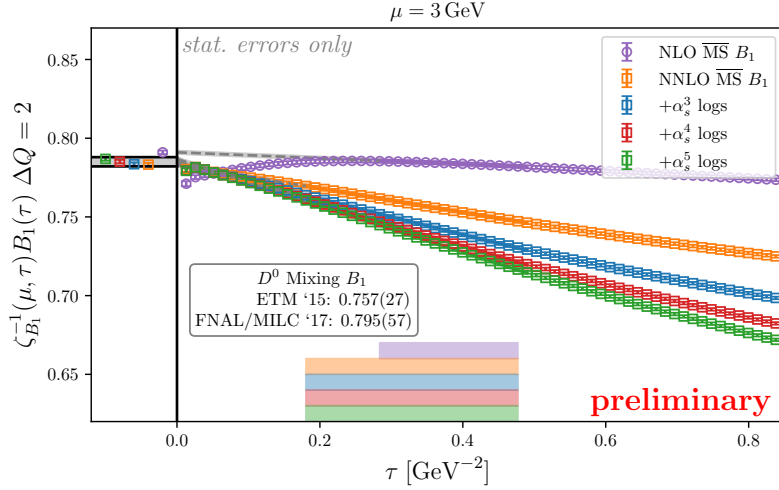


Figure 6: Flow-time dependence of the combination $\zeta_{B_1}^{-1}(\mu, \tau) B_1(\tau)$ with different perturbative orders: NLO (purple), NNLO (orange), $+\alpha_s^3 \text{ logs}$ (blue), $+\alpha_s^4 \text{ logs}$ (red), $+\alpha_s^5 \text{ logs}$ (green). Error bars represent statistical uncertainties only. The gray bands leading from each coloured data set represent the $\tau \rightarrow 0$ extrapolations taken from uncorrelated linear fits; the results at $\tau = 0$ are then shown in the left panel. The coloured bands at the edges of the plots indicate the fit range of τ used for the short-flow-time expansion at each perturbative treatment.

effects of the truncation of perturbation theory. Beyond NNLO, we also include higher-order logarithmic terms of the form $\alpha_s^n \ln^{n-k}(t)$, $k = 0, 1, 2$, which can be derived from renormalisation group considerations. These could be resummed to all orders in n , which we defer to future work. At NLO we choose the flow time window $0.28 \text{ GeV}^{-2} \leq \tau \leq 0.49 \text{ GeV}^{-2}$ and at NNLO (as well as with higher logarithms) we choose $0.18 \text{ GeV}^{-2} \leq \tau \leq 0.49 \text{ GeV}^{-2}$. As can be seen in the figure, the main impact of including higher-order effects in perturbation theory appears to be to extend the region of applicability for the flow time window towards smaller τ .

Since we are simulating a ‘charm-strange’ meson, the $\Delta Q = 2$ bag parameters do not have proper physical meaning. These can however be considered as a proxy to the short-distance effects of

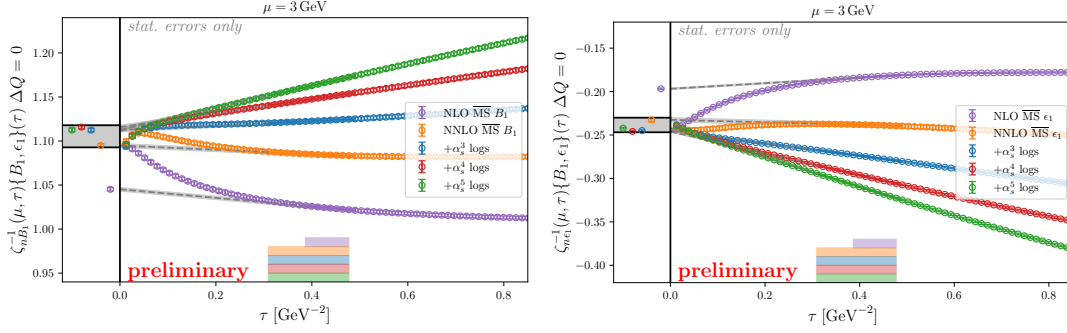


Figure 7: Flow-time dependence of the linear combinations $\zeta_{nm}^{-1}(\mu, \tau)\{B_1, \epsilon_1\}(\tau)$ for $B_1^{\Delta Q=0, \overline{\text{MS}}}$ (left) and $\epsilon_1^{\overline{\text{MS}}}$ (right) using different perturbative orders: NLO (purple), NNLO (orange), $+\alpha_s^3 \text{ logs}$ (blue), $+\alpha_s^4 \text{ logs}$ (red), $+\alpha_s^5 \text{ logs}$ (green). Error bars represent statistical uncertainties only. The gray bands leading from each coloured data set represent the $\tau \rightarrow 0$ extrapolations taken from uncorrelated linear fits; the results at $\tau = 0$ are then shown in the left panel. The coloured bands at the edges of the plots indicate the fit range of τ used for the short-flow-time expansion at each perturbative treatment.

D^0 meson mixing, where we assume spectator effects to be small. In the literature, the short-distance matrix elements for D^0 mixing have been calculated on the lattice by FNAL/MILC at $N_f = 2 + 1$ and ETMC at $N_f = 2 + 1 + 1$, with $\mu = 3 \text{ GeV}$. ETMC finds a value of $B_1^{\overline{\text{MS}}} = 0.757(27)$ [4]. FNAL/MILC quotes a value for $\langle O_1 \rangle^{\overline{\text{MS}}}$ which, using PDG [39], translates to $B_1^{\overline{\text{MS}}} = 0.795(57)$ [5]. There is also a prediction from HQET sum rules, yielding $B_1^{\overline{\text{MS}}} = 0.654^{+0.060}_{-0.052}$ [45]. The preliminary results shown here in figure 6 lie between the two lattice values and slightly above that from HQET sum rules. To incorporate both the statistical uncertainty of the data and the systematic error of truncation in perturbation theory, we take the full spread of the different perturbative treatments at NNLO including higher logs as the range of our final value and choose to symmetrise the errors, yielding

$$B_1^{\Delta Q=2, \overline{\text{MS}}} (3 \text{ GeV}) = 0.785(3). \quad (7)$$

While further systematic uncertainties are still to be included, this agreement with existing values is promising.

Next we consider the $B_1^{\Delta Q=0}$ and ϵ_1 bag parameters. Although the continuum limit at fixed flow time avoids mixing with lower-dimensional operators, power divergences may still emerge in the SFTX; see e.g. Ref. [46]. We plan to address this issue in the future. In the meantime, we use the perturbative matching calculated for the difference of $\Delta Q = 0$ operators with different spectator quarks, where the troublesome terms cancel. The combinations of the matching matrices and the continuum-limit lattice data are shown in figure 7 for $B_1^{\Delta Q=0, \overline{\text{MS}}}$ and $\epsilon_1^{\overline{\text{MS}}}$. For both bag parameters, the flow time windows $0.39 \text{ GeV}^{-2} \leq \tau \leq 0.48 \text{ GeV}^{-2}$ at NLO and $0.31 \text{ GeV}^{-2} \leq \tau \leq 0.48 \text{ GeV}^{-2}$ at NNLO are chosen. To date no lattice QCD determination with a full error budget exists, only sum rules computations in HQET [45]. We thus decided to compare with the HQET sum rules results for lifetime differences matched to full QCD, which give $B_1^{\Delta Q=0} = 0.902^{+0.077}_{-0.051}$ and $\epsilon_1 = -0.132^{+0.041}_{-0.046}$ [45]. At the preliminary stages of our calculation, again incorporating the full

spread of the different perturbative treatments at NNLO into the final values, we find

$$B_1^{\Delta Q=0, \overline{\text{MS}}}(3 \text{ GeV}) = 1.105(13), \quad \text{and} \quad \epsilon_1^{\overline{\text{MS}}}(3 \text{ GeV}) = -0.239(8), \quad (8)$$

and we observe that both $B_1^{\Delta Q=0}$ and ϵ_1 lie relatively close to the predictions for lifetime differences based on sum rules.

4. Summary

For quantities deduced using the heavy quark expansion, $\Delta B = 0$ four-quark matrix elements play an important role in improving precision and accuracy. However, these are not yet determined using lattice QCD. One of the difficulties impeding their calculation is mixing with lower-dimension operators. We have here demonstrated the use of the gradient flow to non-perturbatively calculated renormalised matrix elements of four-quark operators. We convert the results at finite flow time to the $\overline{\text{MS}}$ scheme by performing a perturbative matching using the SFTX. Preliminary results have been obtained for D_s mesons. While we consider both $\Delta Q = 2$ and $\Delta Q = 0$ operators, only $\Delta Q = 0$ have a direct physical meaning. A full systematic error analysis is yet to be undertaken.

Calculating $\Delta Q = 2$ bag parameters is well-established and provides a test case for our method where findings can be compared to results for short-distance D^0 mixing, assuming spectator effects to be negligible. We find good agreement between our results and literature values. Furthermore, we have made first steps towards predictions for the $\Delta Q = 0$ bag parameters. While additional operators and diagrams are still required in both the lattice calculation and perturbative matching, we observe that our preliminary results have the expected order of magnitudes.

Acknowledgments

These computations used resources provided by the OMNI cluster at the University of Siegen, the HAWK cluster at the High-Performance Computing Center Stuttgart, and LUMI-G at the CSC data center Finland (DeiC National HPC g.a. DEIC-SDU-L5-13 and DEIC-SDU-N5-2024053). We thank the RBC/UKQCD collaboration for generating and making their gauge ensembles publicly available. M.B., R.H., O.W. received support from the Deutsche Forschungsgemeinschaft (DFG, German Research Foundation) through grant 396021762 - TRR 257 “Particle Physics Phenomenology after the Higgs Discovery”. A.S. received support from the DFG through grant 513989149, the National Science Foundation grant PHY-2209185 and the DOE Topical Collaboration “Nuclear Theory for New Physics” award No. DE-SC0023663. The work of F.L. was supported by the Swiss National Science Foundation (SNSF) under contract [TMSGI2_211209](#). Special thanks is given to Felix Erben, Ryan Hill, and J. Tobias Tsang for assistance in setting up the simulation code.

Comment

After submitting the original version of this proceedings to arXiv, we discovered a mistake in our analysis for the lifetimes which has been corrected in version 2 and the resulting values for $B_1^{\Delta Q=0}$ and ϵ_1 have been updated.

References

- [1] Heavy Flavor Averaging Group, HFLAV collaboration, Y. S. Amhis et al., *Averages of b -hadron, c -hadron, and τ -lepton properties as of 2021*, *Phys. Rev. D* **107** (2023) 052008 [[arXiv:2206.07501](#)].
- [2] J. Albrecht et al., *Lifetimes of b -hadrons and mixing of neutral B -mesons: theoretical and experimental status*, *Eur. Phys. J. ST* **233** (2024) 359 [[arXiv:2402.04224](#)].
- [3] N. Carrasco et al., *$D^0 - \bar{D}^0$ mixing in the standard model and beyond from $N_f=2$ twisted mass QCD*, *Phys. Rev. D* **90** (2014) 014502 [[arXiv:1403.7302](#)].
- [4] ETM collaboration, N. Carrasco, P. Dimopoulos, R. Frezzotti, V. Lubicz, G. C. Rossi, S. Simula et al., *$\Delta S=2$ and $\Delta C=2$ bag parameters in the standard model and beyond from $N_f=2+1+1$ twisted-mass lattice QCD*, *Phys. Rev. D* **92** (2015) 034516 [[arXiv:1505.06639](#)].
- [5] A. Bazavov et al., *Short-distance matrix elements for D^0 -meson mixing for $N_f = 2 + 1$ lattice QCD*, *Phys. Rev. D* **97** (2018) 034513 [[arXiv:1706.04622](#)].
- [6] ETM collaboration, N. Carrasco et al., *B -physics from $N_f = 2$ tmQCD: the Standard Model and beyond*, *JHEP* **03** (2014) 016 [[arXiv:1308.1851](#)].
- [7] RBC collaboration, Y. Aoki, T. Ishikawa, T. Izubuchi, C. Lehner and A. Soni, *Neutral b meson mixings and b meson decay constants with static heavy and domain-wall light quarks*, *Phys.Rev.D* **91** (2015) 114505 [[arXiv:1406.6192](#)].
- [8] HPQCD collaboration, E. Gamiz et al., *Neutral B Meson Mixing in Unquenched Lattice QCD*, *Phys. Rev. D* **80** (2009) 014503 [[arXiv:0902.1815](#)].
- [9] Fermilab/MILC collaboration, A. Bazavov et al., *$B_{(s)}^0$ -mixing matrix elements from lattice qcd for the standard model and beyond*, *Phys.Rev.D* **93** (2016) 113016 [[arXiv:1602.03560](#)].
- [10] HPQCD collaboration, R. Dowdall, C. Davies, R. Horgan, G. Lepage, C. Monahan, J. Shigemitsu et al., *Neutral b -meson mixing from full lattice qcd at the physical point*, *Phys.Rev.D* **100** (2019) 094508 [[arXiv:1907.01025](#)].
- [11] P. Boyle, F. Erben, A. Jüttner, T. Kaneko, M. Marshall, A. Portelli et al., *BSM $B - \bar{B}$ mixing on JLQCD and RBC/UKQCD $N_f = 2 + 1$ DWF ensembles*, *PoS LATTICE2021* (2022) 224 [[arXiv:2111.11287](#)].
- [12] UKQCD collaboration, M. Di Pierro and C. T. Sachrajda, *A Lattice study of spectator effects in inclusive decays of B mesons*, *Nucl. Phys. B* **534** (1998) 373 [[arXiv:hep-lat/9805028](#)].
- [13] UKQCD collaboration, M. Di Pierro, C. T. Sachrajda and C. Michael, *An Exploratory lattice study of spectator effects in inclusive decays of the Λ_b baryon*, *Phys. Lett. B* **468** (1999) 143 [[arXiv:hep-lat/9906031](#)], [Erratum: *Phys.Lett.B* 525, 360–360 (2002)].
- [14] D. Becirevic, *Theoretical progress in describing the B meson lifetimes*, *PoS HEP2001* (2001) 098 [[arXiv:hep-ph/0110124](#)].
- [15] J. Lin, W. Detmold and S. Meinel, *Lattice Study of Spectator Effects in b -hadron Decays*, *PoS LATTICE2022* (2023) 417 [[arXiv:2212.09275](#)].
- [16] M. Black et al., *Using Gradient Flow to Renormalise Matrix Elements for Meson Mixing and Lifetimes*, *PoS LATTICE2023* (2024) 263 [[arXiv:2310.18059](#)].

- [17] M. Black, *Improving Precision for Hadronic Observables in the Standard Model and Beyond*, Ph.D. thesis, Universität Siegen, 2024. <http://dx.doi.org/10.25819/ubsi/10603>.
- [18] R. Narayanan and H. Neuberger, *Infinite N phase transitions in continuum Wilson loop operators*, *JHEP* **03** (2006) 064 [[arXiv:hep-th/0601210](#)].
- [19] M. Lüscher, *Properties and uses of the Wilson flow in lattice QCD*, *JHEP* **08** (2010) 071 [[arXiv:1006.4518](#)], [Erratum: *JHEP* **03**, 092 (2014)].
- [20] M. Lüscher, *Chiral symmetry and the Yang–Mills gradient flow*, *JHEP* **04** (2013) 123 [[arXiv:1302.5246](#)].
- [21] M. Lüscher and P. Weisz, *Perturbative analysis of the gradient flow in non-abelian gauge theories*, *JHEP* **02** (2011) 051 [[arXiv:1101.0963](#)].
- [22] H. Suzuki, *Energy–momentum tensor from the Yang–Mills gradient flow*, *PTEP* **2013** (2013) 083B03 [[arXiv:1304.0533](#)], [Erratum: *PTEP* **2015**, 079201 (2015)].
- [23] M. Lüscher, *Future applications of the Yang–Mills gradient flow in lattice QCD*, *PoS LATTICE2013* (2014) 016 [[arXiv:1308.5598](#)].
- [24] T. Endo, K. Hieda, D. Miura and H. Suzuki, *Universal formula for the flavor non-singlet axial-vector current from the gradient flow*, *PTEP* **2015** (2015) 053B03 [[arXiv:1502.01809](#)], [Erratum: *PTEP* **2024**, 039202 (2024)].
- [25] K. Hieda and H. Suzuki, *Small flow-time representation of fermion bilinear operators*, *Mod. Phys. Lett. A* **31** (2016) 1650214 [[arXiv:1606.04193](#)].
- [26] R. V. Harlander and F. Lange, *Effective electroweak Hamiltonian in the gradient-flow formalism*, *Phys. Rev. D* **105** (2022) L071504 [[arXiv:2201.08618](#)].
- [27] J. Borgulat et al., *Short-flow-time expansion of quark bilinears through next-to-next-to-leading order QCD*, *JHEP* **05** (2024) 179 [[arXiv:2311.16799](#)].
- [28] RBC/UKQCD collaboration, T. Blum et al., *Domain wall QCD with physical quark masses*, *Phys. Rev. D* **93** (2016) 074505 [[arXiv:1411.7017](#)].
- [29] RBC/UKQCD collaboration, P. A. Boyle, L. Del Debbio, A. Jüttner, A. Khamseh, F. Sanfilippo and J. T. Tsang, *The decay constants f_D and f_{D_s} in the continuum limit of $N_f = 2 + 1$ domain wall lattice QCD*, *JHEP* **12** (2017) 008 [[arXiv:1701.02644](#)].
- [30] RBC/UKQCD collaboration, P. A. Boyle, L. Del Debbio, N. Garron, A. Jüttner, A. Soni, J. T. Tsang et al., *$SU(3)$ -breaking ratios for $D_{(s)}$ and $B_{(s)}$ mesons*, [arXiv:1812.08791](#).
- [31] D. B. Kaplan, *A Method for simulating chiral fermions on the lattice*, *Phys. Lett. B* **288** (1992) 342 [[arXiv:hep-lat/9206013](#)].
- [32] Y. Shamir, *Chiral fermions from lattice boundaries*, *Nucl. Phys. B* **406** (1993) 90 [[arXiv:hep-lat/9303005](#)].
- [33] V. Furman and Y. Shamir, *Axial symmetries in lattice QCD with Kaplan fermions*, *Nucl. Phys. B* **439** (1995) 54 [[arXiv:hep-lat/9405004](#)].
- [34] T. Blum and A. Soni, *QCD with domain wall quarks*, *Phys. Rev. D* **56** (1997) 174 [[arXiv:hep-lat/9611030](#)].

- [35] RBC/UKQCD collaboration, C. Allton et al., *Physical Results from 2+1 Flavor Domain Wall QCD and SU(2) Chiral Perturbation Theory*, *Phys. Rev.* **D78** (2008) 114509 [[arXiv:0804.0473](#)].
- [36] RBC/UKQCD collaboration, Y. Aoki et al., *Continuum Limit Physics from 2+1 Flavor Domain Wall QCD*, *Phys.Rev.* **D83** (2011) 074508 [[arXiv:1011.0892](#)].
- [37] C. Morningstar and M. J. Peardon, *Analytic smearing of SU(3) link variables in lattice QCD*, *Phys. Rev. D* **69** (2004) 054501 [[arXiv:hep-lat/0311018](#)].
- [38] R. C. Brower, H. Neff and K. Orginos, *The Möbius domain wall fermion algorithm*, *Comput. Phys. Commun.* **220** (2017) 1 [[arXiv:1206.5214](#)].
- [39] Particle Data Group collaboration, R. L. Workman and Others, *Review of Particle Physics*, *PTEP* **2022** (2022) 083C01.
- [40] P. Boyle, G. Cossu, A. Portelli and A. Yamaguchi, [github.com/paboyle/Grid](#): Grid.
- [41] P. A. Boyle, G. Cossu, A. Yamaguchi and A. Portelli, *Grid: A next generation data parallel C++ QCD library*, *PoS LATTICE2015* (2016) 023.
- [42] A. Portelli, R. Abbott, N. Asmussen, A. Barone, P. A. Boyle, F. Erben et al., [github.com/aportelli/hadrons](#): *Hadrons v1.3*, Mar., 2022. 10.5281/zenodo.6382460.
- [43] RBC, UKQCD collaboration, P. A. Boyle et al., *Simulating rare kaon decays $K^+ \rightarrow \pi^+ \ell^+ \ell^-$ using domain wall lattice QCD with physical light quark masses*, *Phys. Rev. D* **107** (2023) L011503 [[arXiv:2202.08795](#)].
- [44] D. King, A. Lenz and T. Rauh, *SU(3) breaking effects in B and D meson lifetimes*, *JHEP* **06** (2022) 134 [[arXiv:2112.03691](#)].
- [45] M. Kirk, A. Lenz and T. Rauh, *Dimension-six matrix elements for meson mixing and lifetimes from sum rules*, *JHEP* **12** (2017) 068 [[arXiv:1711.02100](#)], [Erratum: *JHEP* **06**, 162 (2020)].
- [46] SymLat collaboration, J. Kim, T. Luu, M. D. Rizik and A. Shindler, *Nonperturbative renormalization of the quark chromoelectric dipole moment with the gradient flow: Power divergences*, *Phys. Rev. D* **104** (2021) 074516 [[arXiv:2106.07633](#)].